Desalination and Water Treatment
www.deswater.com
41 (2012) 224–231
March
1944-3994/1944-3986 © 2012 Desalination Publications. All rights reserved
doi: 10.1080/19443994.2012.664717
Taylor & Francis
Taylor & Francis Group

Color and COD reduction from cotton textile processing wastewater by activated carbon derived from solid waste in column mode

A.A. Ahmad[a,*], A. Idris[a], B.H. Hameed[b]

[a]*Department of Chemical and Environmental Engineering, Faculty of Engineering, University Putra Malaysia, 43400 UPM, Serdang, Malaysia*
Tel. +603 89466302; Fax: +60 3 86567120; email: abdulbari@eng.upm.edu.my
[b]*School of Chemical Engineering, Engineering Campus, University Science of Malaysia, 14300 Nibong Tebal, Penang, Malaysia*

Received 27 July 2011; Accepted 17 January 2012

ABSTRACT

Rattan-activated carbon was evaluated for color reduction and chemical oxygen demand (COD) of a cotton textile mill wastewater in a fixed-bed adsorption column. The maximum adsorption capacities of color and COD were 100.15 Pt/Co and 73.23 mg/L, respectively, at 10 mL/min flow rate and 80 mm bed height. Kinetic models, Adams–Bohart, Thomas and Yoon–Nelson were applied to experimental data to predict the breakthrough curves using linear regression. The Thomas and Yoon–Nelson models were found suitable for the description of the breakthrough curve while the Adams–Bohart model was only used to predict the initial part of the dynamic process. The results of this study indicated the applicability of fixed-bed column for reduction of color and COD from textile mill wastewater.

Keywords: Rattan waste; Activated carbon; Textile wastewater; Fixed-bed column; Adsorption; Modeling

1. Introduction

Wastewater discharged by industrial activities is often contaminated by a variety of toxic or other harmful substances which have negative effects on the water environment [1]. For example, the cotton textile that processes wastewater generated by the different production steps (i.e. sizing of fibers, scouring, desizing, bleaching, washing, mercerization, dyeing, and finishing) has high pH, temperature, detergents, oil, suspended and dissolved solids, toxic and non-biodegradable matter, color, chemical oxygen demand (COD), and alkalinity [2,3]. Biological treatment process is generally efficient in biological oxygen demand (BOD) and suspended solids removal; however, it is considered unsatisfactory because of the low biodegradability and low reaction rate of treatment [4]. With different types of activated sludge treatment methods, the following removals (90% of BOD, 40–50% of COD and 10–30% of color) are normally achieved [5–7].

Adsorption onto activated carbon has been found to be superior for wastewater treatment compared to other physical and chemical techniques such as flocculation, coagulation, precipitation, and ozonation as they possess inherent limitations such as high cost, formation of hazardous by-products, and intensive energy requirements [8]. However, commercially

*Corresponding author.

available activated carbons are still considered expensive [9]. This is due to the use of non-renewable and relatively expensive starting material such as coal, which is unjustified in pollution control applications [10]. Therefore, in recent years, this has prompted a growing research interest in the production of activated carbons from renewable and cheaper precursors, which are mainly agricultural by-products such as cotton stalk [11], husk [12], jackfruit peel [13], oil palm shell [14], bamboo waste [15].

Batch reactor was easy to use in the laboratory study, but less convenient for industrial applications. On the other hand, fixed-bed column was widely used in various chemical industries because of their operation [16]. To predict the breakthrough curve of a fixed bed with a sophisticated mass transfer model, one needs many parameters that must be determined by independent batch kinetic study or estimated by suitable correlations [17–19]. Mathematical models facilitate the design and analysis of full-scale systems by reducing the number of pilot-scale test required to evaluate various operating conditions and design parameters for adsorption. The design of the adsorption process is based on the accurate production of breakthrough curves. Various mathematical models have been developed to describe contaminant adsorption onto different adsorbents in many of the diverse applications for which the adsorbents are used [20,21].

The objective of this work to evaluate the efficiency of Rattan-activated carbon (RAC) for reducing color and COD for the aerobically treated effluent from the cotton textile mill wastewater in fixed-bed column. Thomas, Adams–Bohart, and Yoon–Nelson models were used to describe the adsorption kinetics in column.

2. Materials and methods

2.1. Sampling

Wastewater samples were maintained from one factory discharge point after aerobically treated. These samples were collected from a cotton textile mill in Penang State, Malaysia. The samples were stored at $\leqslant 5$ °C to avoid any change in their physico-chemical characteristics before use. The current wastewater treatment scheme at the site consists of screening, preneutralization, anaerobic lagoon, post-neutralization, activated sludge process, and sedimentation. However, the treated wastewater is still unable to meet the local discharge limit (MDC, 1997) [22], especially in terms of color and COD. The characterization of textile wastewater (final effluent after biological treatment) and standard B refer to discharge limit in terms of color and COD in Malaysia with reference to our previous work [9]. The wastewater samples were analyzed in our laboratory according to the methods prescribed in APHA [23].

2.2. Preparation of activated carbon

Rattan waste (RW) used for preparation of activated carbon was collected from a local furniture shop, Penang State, Malaysia. The procedure used to prepare the activated carbon was referred to in our previous work [24]. Briefly, the RW was washed with hot distilled water to remove dust-like impurities, dried at 105°C, grounded, and sieved (400–600 μm) to discrete sizes. Activation of the phosphoric acid-impregnated precursor was carried out at a temperature of 500°C for 2 h under purified nitrogen (99.995%) flow (150 cm^3/g) at a heating rate of 10°C/min in a horizontal tubular furnace. After activation, the sample was cooled down to room temperature with the same heating rate and washed sequentially several times with hot distilled water (70°C) until the pH of the washing solution reached 6–7. Finally, the sample was dried in an oven at 110°C for 24 h and then stored in plastic containers.

Textural characterization of the RAC was carried out by N_2 adsorption at 77 K using ASAP 2020 Micromeritics by Brunauer–Emmett–Teller (BET) method, using the software of Micromeritics. Surface morphology and the presence of porosity of the activated carbon prepared in this work were studied using scanning electron microscopy (SEM) analysis. The surface functional group of the RAC was detected by Fourier Transform Infrared (FTIR) spectroscope (FTIR-2000, PerkinElmer).

2.3. Experimental set-up

Continuous flow adsorption studies were conducted in a glass column made of Pyrex glass tube of 1.2 cm inner diameter and 19.5 cm height. At the bottom of the column, a stainless sieve (150 μm) was attached followed by a layer of glass wool. A known quantity of the RAC was packed in the column to yield the desired bed height of activated carbon 40, 60, and 80 mm equivalent to 1.23, 1.85, and 2.41 g of activated carbon, respectively. The column was then filled up with glass beads (2 mm diameter) in order to provide a uniform flow of the solution through the column. The initial COD and color were fixed at 251.65 mg/L and 486.87 Pt/Co, respectively. The COD and color were pumped upward through the column at a desired flow rate (10, 20 and 30 mL/min) con-

trolled by a peristaltic pump (Masterflex, Cole-Parmer Instrument Co.). The samples were analyzed using DR2800 spectrophotometer (CECIL 1000 series, Cambridge, UK) at wavelengths of 620 nm and 455 nm for COD and color, respectively. All the experiments were carried out at room temperature (28 ± 1°C). Total adsorbed color and COD quantity q_{total} (mg) in the column for a given feed concentration and flow rate is calculated as [25].

$$q_{total} = \frac{Q}{1000}\int_{t=o}^{t=t_{total}} C_{ad}dt \quad (1)$$

Equilibrium uptake q_{eq} (mg/g) or maximum capacity of the column in the column is defined by Eq. (2) as the total amount of adsorbed (q_{total}) per gram of adsorbent (w) at the end of total flow time [25].

$$q_{eq} = \frac{q_{total}}{w} \quad (2)$$

3. Modeling of column

3.1. Breakthrough curves

Successful design of an adsorption column requires prediction of the concentration–time profile from breakthrough curve for the effluent discharged from the column [26]. The maximum adsorption capacity of an adsorbent is also needed in the design of an adsorbent column. The performance of a fixed-bed column is obtained through the concept of breakthrough curve. In many cases, kinetics of adsorption in column has been tested for Bohart–Adams model [27]. However, it has also been shown that Thomas [28] and Yoon–Nelson models [29] can sometimes provide a better description of the adsorption kinetics.

3.2. Thomas model

Thomas model [28] is one of the most general and widely used models in the column performance theory. The expression developed by Thomas determines the maximum solid phase concentration of solute on the adsorbent and the adsorption rate constant for an adsorption process in column. The linearized form of the model is expressed as:

$$\ln\left(\frac{C_o}{C_t} - 1\right) = \frac{k_{Th}q_o w}{Q} - k_{Th}C_0 t \quad (3)$$

where k_{Th} (mL/min mg) is the Thomas rate constant, q_o (mg/g) is the equilibrium effluent uptake per g of the adsorbent, C_o (mg/L) is the inlet effluent concentration; C_t (mg/L) is the outlet concentration at time t; W (g) the mass of adsorbent, Q (mL/min) the flow rate, and t_{total} (min) stands for flow time. The value of C_t/C_o is the ratio of outlet and inlet effluent concentrations. A linear plot of $\ln[(C_o/C_t) - 1]$ against time (t) was employed to determine values of k_{Th} and q_o from the intercepts and slopes of the plot.

3.3. Adams–Bohart model

Adams–Bohart model [27] assumes that the adsorption rate is proportional to both the residual capacity of the adsorbent and the concentration of the adsorbing species. The Bohart–Adams model was used for the initial part of the breakthrough curve [25]. Its overall approach is now being applied successfully in quantitative description of other systems. The mathematical equation of the model can be written as:

$$\ln\frac{C_t}{C_o} = k_{AB}C_o t - k_{AB}N_o\frac{Z}{F} \quad (4)$$

where, C_o and C_t (mg/L) are the inlet and effluent concentration. k_{AB} (L/mg min) is the kinetic constant, F (cm/min) is the linear velocity calculated by dividing the flow rate by the column section area, Z (cm) is the bed depth of column, and N_o (mg/L) is the saturation concentration. A linear plot of $\ln C_t/C_o$ against time (t) was employed to determine the values of k_{AB} and N_o from the intercepts and slopes of the plot.

3.4. Yoon–Nelson model

Yoon and Nelson [29] have developed a relatively simple model addressing the adsorption and breakthrough of adsorbate gases with respect to activated charcoal. This model was derived based on the assumption that the rate of decrease in the probability of adsorption for each adsorbate molecule is proportional to the probability of adsorbate adsorption and the probability of adsorbate breakthrough on the adsorbent. The linearized model for a single component system is expressed as:

$$\ln\frac{C_t}{C_o - C_t} = k_{YN}t - \tau k_{YN} \quad (5)$$

where k_{YN} (1/min) is the rate velocity constant, τ (min) is the time required for 50% adsorbate breakthrough. A linear plot of $\ln[C_t/(C_o - C_t)]$ against sampling time (t) was employed to determine the values of k_{YN} and τ from the intercept and slope of the plot.

3.5. The error analysis

The average percentage errors ($\varepsilon\%$) are used to indicate the fit between the experimental and theoretical values of C_t/C_o used for plotting breakthrough curves and they are calculated using the following equation [16]:

$$\varepsilon = \frac{\sum_{i=1}^{N}\left[((C_t/C_o)_{exp} - (C_t/C_o)_{theo})/(C_t/C_o)_{exp}\right]}{N} \times 100 \quad (6)$$

where N is the number of measurements. The lowest value of $\varepsilon\%$ indicates the best model to represent the experimental data.

4. Results and discussion

4.1. Characterization of activated carbon

The activated carbon prepared from RW under the optimum conditions was found to have well-developed pores on its surface and high surface area was referred to our previous work [24]. From the SEM image obtained, large and well-developed pores were clearly found on the surface of the activated carbon. The BET surface area of the prepared activated carbon was 1037.18 m^2/g and various functional groups on the prepared activated carbon were determined from the FTIR results [24].

4.2. Effect of flow rate

The effect of flow rate on the adsorption of color and COD in the fixed bed with a bed depth of 19.5 cm was investigated. The flow rate was changed in the range of 10, 20, and 30 mL/min while the initial color and COD concentrations were fixed at 486.87 Pt/Co and 251.65 mg/L, respectively. The experimental breakthrough times for color (corresponding to $C/C_o = 0.01$) and COD (corresponding to $C/C_o = 0.02$) were observed as 15, 10, and 5 min. Table 1 shows the complete bed exhaustion time (min) for color and COD at flow rates and bed height (corresponding to $C/C_o = 1.0$). The adsorption breakthrough curves of color and COD obtained at different flow rates are shown in Fig. 1a and b. The column was found to perform better at a lower linear flow rate which resulted in a longer breakthrough and exhaustion time. At a higher linear flow rate, the adsorption capacities were lower due to insufficient residence time of the solute in the column and diffusion of the solute into the pores of the adsorbent, and therefore, the solute left the column before equilibrium occurred. These results are in agreement with those referred to in the literatures [14,30,31].

4.3. Effect of bed height

The adsorption capacity of fixed-bed column with bed height of 40, 60 and 80 mm (equivalent to 1.23, 1.85, and 2.41 g) were tested at a constant flow rate of 10 mL/min and the constant influent concentration of 486.87 Pt/Co color and 251.65 mg/L of COD. The breakthrough curves of color and COD are illustrated in Fig. 2a and b. The complete bed exhaustion times (min) breakthrough were 60, 70, 90 min for color and 45, 50, 70 min for COD at the bed depth of 40, 60, and 80 mm, respectively (Table 1) suggesting that the breakthrough time increased with bed height. Moreover, an increase in the bed adsorption capacity (q_{eq}) is noticed at the breakthrough point with the increase in bed height (Table 1). Besides, a delayed breakthrough of the pollutant leads to an increase in the volume of the solution treated. The increase in adsorption with that in bed height was due to the increase in adsorbent doses in larger beds which provide greater surface area (or adsorption sites) [32,33]. The breakthrough time

Table 1
Column data parameters obtained at different flow rates and bed heights (initial color concentration 486.87 Pt/Co, Initial COD concentration 251.65 mg/L, pH = 4, and $T = 28 \pm 1$°C)

Flow rate (mL/min)	RAC bed height (mm)	Color		COD	
		Complete bed exhaustion time (min)	q_e	Complete bed exhaustion time (min)	q_e
10	60	70	89.21	50	55.08
20	60	50	72.63	45	38.22
30	60	35	28.46	30	20.17
10	40	60	42.9	45	40.17
10	80	90	100.15	70	73.23

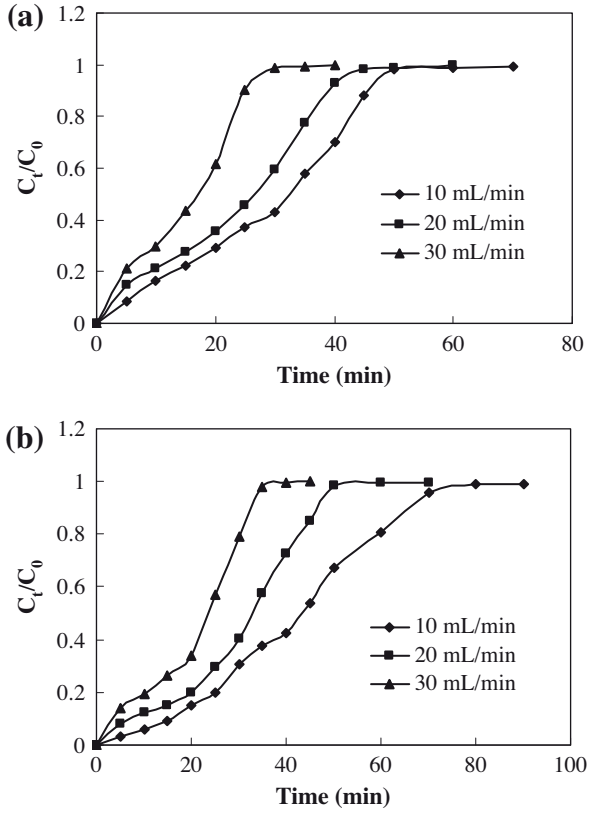

Fig. 1. Breakthrough curves for (a) color, (b) COD adsorption on RAC at different flow rates (initial color concentration 486.87 Pt/C_o, initial COD concentration 251.65 mg/L, pH = 4, and $T = 28 \pm 1$°C).

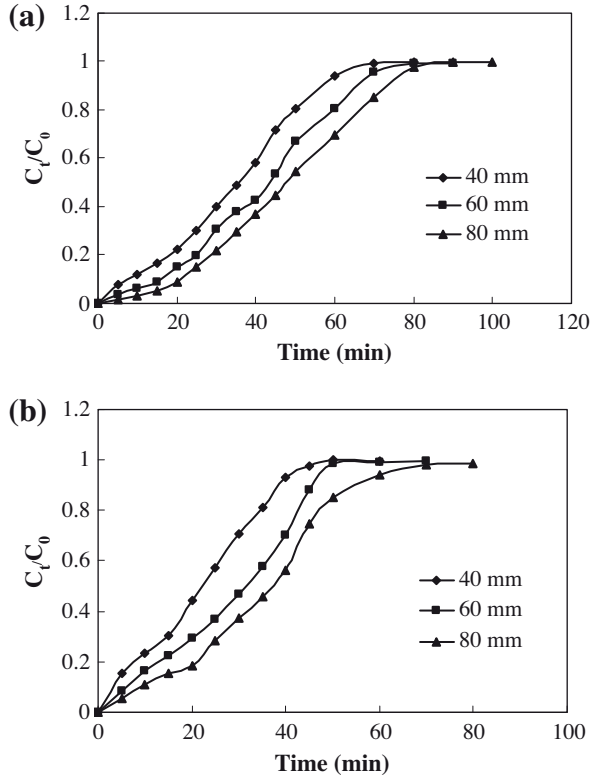

Fig. 2. Breakthrough curves for (a) color, (b) COD adsorption on RAC at different bed heights (initial color concentration 486.87 Pt/C_o, initial COD concentration 251.65 mg/L, pH = 4, and $T = 28 \pm 1$°C).

also increased with the height of the bed. The larger it is, the better the intra-particulate phenomena and the bed adsorption capacity are (Table 1). The results obtained in this study are similar to those in studies concerned with the elimination of congo red by using rice husk [34].

4.4. Thomas model

The experimental data were fitted to the Thomas model to determine the Thomas rate constant (k_{Th}) and maximum solid phase concentration (q_o). The k_{Th} and q_0 value were calculated by plotting $\ln(C_o/C_t - 1)$ against t (figure not shown) using values from the column experiments. From the correlation coefficient (R^2) and other statistical parameters, it can be concluded that the experimental data fitted well to the Thomas model. The values of k_{Th}, q_o and the correlation coefficients at all flow rates and bed height studied are summarized in Table 2. The determined coefficients and Thomas rate constant are obtained using linear regression analysis according to Eq. (4). They were all fitting with higher determined coefficients (R^2) ranging from 0.83 to 0.91 for color and 0.79 to 0.88 for COD and average percentage errors (ε%) less than 5.86 both color and COD. As the flow rate increased, the k_{Th} value increased for both color and COD, whereas the value of q_o showed a reverse trend, i.e. decreased with increase in the flow rate (Table 2). As the bed height increased, the value of q_0 increased significantly while the value of k_{Th} decreased significantly for both color and COD. Therefore, a higher flow rate and a lower bed height have a disadvantage towards adsorption of color and COD on RAC column. A similar trend has also been observed by Aksu and Gonen [25]. The well fit of the experimental data onto the Thomas model indicates that the external and internal diffusion will not be the limiting step [35].

4.5. Adams–Bohart model

The Adams–Bohart adsorption model was applied to the experimental data for the description of the initial part of the breakthrough curve. The values of k_{AB} and N_o calculated from the $\ln(C_t/C_o)$ vs. t plots (figure not shown) at all flow rates and bed height studied are presented in Table 3 together with the correlation

Table 2
Thomas model parameters for fixed-bed adsorption of color and COD on RAC (initial color concentration 486.87 Pt/Co, initial COD concentration 251.65 mg/L, pH = 4, and $T = 28 \pm 1$°C)

Flow rate (mL/min)	RAC bed height (mm)	Color				COD			
		$k_{Th} \times 10^3$	q_o	R^2	ε (%)	$k_{Th} \times 10^3$	q_o	R^2	ε (%)
10	60	0.173	60.82	0.91	2.87	0.37	50.01	0.86	3.41
20	60	0.227	30.27	0.86	3.53	0.43	41.72	0.85	3.71
30	60	0.461	29.51	0.83	5.86	0.69	31.94	0.87	3.35
10	40	0.196	81.30	0.91	2.64	0.33	27.71	0.79	5.09
10	80	0.191	106.27	0.87	1.92	0.29	37.23	0.88	2.41

Table 3
Adams–Bohart model parameters for fixed-bed adsorption of color and COD on RAC (initial color concentration 486.87 Pt/Co, initial COD concentration 251.65 mg/L, pH = 4, and $T = 28 \pm 1$°C)

Flow rate (mL/min)	RAC bed height (mm)	Color				COD			
		$k_{AB} \times 10^3$	N_o	R^2	ε (%)	$k_{AB} \times 10^3$	N_o	R^2	ε (%)
10	60	0.471	205.93	0.52	10.25	0.059	141.8	0.47	12.23
20	60	0.524	176.21	0.48	9.07	0.074	110.81	0.46	21.71
30	60	0.607	112.34	0.42	12.99	0.086	67.12	0.41	23.02
10	40	0.404	87.77	0.51	11.09	0.512	82.26	0.42	14.98
10	80	0.053	195.06	0.53	8.69	0.068	122.75	0.49	13.84

coefficients and average percentage errors (ε%). As seen from Table 3, both the kinetic constant k_{AB} and maximum adsorption capacity N_o were affected by flow rate and bed height of color and COD. The values of k_{AB} increased with increasing flow rate and decreased with increasing bed height for color and COD. As expected, the maximum adsorption capacity (N_o) decreased with increasing flow rate and increased with increasing bed height of color and COD. The Adams–Bohart model did not give better fits with higher determined coefficients (R^2), which was less than 0.53 and higher values of average percentage errors (ε%) for both color and COD. Although the original work by Adams–Bohart was done for the gas–charcoal adsorption system, its overall approach has been applied successfully in quantitative description of other systems [36,37]. In this model, the adsorption rate is assumed to be proportional to both residual capacity of activated carbon and concentration of the adsorbing species. The mass transfer coefficient (k_{AB}) and saturation concentration (N_o) values were calculated from the slope and intercept of the curve, respectively. As shown in Table 3, it is observed that mass transfer coefficient increased with an increase in flow rate. This showed that the overall system kinetics was dominated by external mass transfer [25].

4.6. Yoon–Nelson model

A simple theoretical model developed by Yoon–Nelson was applied to investigate the breakthrough behavior of color and COD on the RAC. The values of k_{YN} and were estimated from the graph between $\ln(C_t/C_0 - C_t)$ vs. t (figure not shown) at different flow rates and bed height. The values of k_{YN} and τ were determined at different flow rates varied between 10, 20, and 30 mL/min, at different bed height 40, 60, 80 mm and fixed inlet concentration 486.87 Pt/Co of color and 251.65 mg/L of COD. These values were used to calculate the breakthrough curve. From linearized Yoon–Nelson equation plots, the correlation coefficients (R^2), average percentage errors (ε%), k_{YN} and τ_{cal} were calculated for tested experimental parameters and they are shown in Table 4. As shown in Table 4, k_{YN} increased with increasing flow rate and decreased with an increase in the bed height at both color and COD. As for τ, it decreased with an increase in flow rate and increased with an increase in bed height of RAC for color and COD. As shown in Table 4, it can be seen that simulation of the whole breakthrough curve is effective with the Yoon–Nelson model at lower flow rate and at higher bed height.

Table 4
Yoon–Nelson model parameters for fixed-bed adsorption of color and COD on RAC (initial color concentration 486.87 Pt/Co, initial COD concentration 251.65 mg/L, pH = 4, and $T = 28 \pm 1$°C)

Flow rate (mL/min)	RAC bed height (mm)	Color				COD			
		k_{YN}	τ	R^2	ε (%)	k_{YN}	τ	R^2	ε (%)
10	60	0.084	36.93	0.91	1.08	0.089	24.78	0.67	5.27
20	60	0.119	25.07	0.85	2.03	0.114	18.75	0.79	3.87
30	60	0.177	15.26	0.83	3.36	0.173	10.24	0.87	2.76
10	40	0.094	28.75	0.91	1.79	0.084	13.49	0.97	1.97
10	80	0.091	41.18	0.89	2.81	0.074	30.7	0.88	2.61

4.7. Comparison of Thomas, Adams–Bohart and Yoon–Nelson models

Comparing the values of average percentage errors (ε%) in Thomas, Adams–Bohart, and Yoon–Nelson models in Tables 2–4, the values of average percentage errors (ε%) in Thomas model and Yoon–Nelson were lower than those in Adams–Bohart. Thus, it was concluded that the Thomas and Yoon–Nelson models can be used to describe the behavior of the adsorption process, but the Adams–Bohart model did not give better results. Adams–Bohart model is only used to predict the initial region of breakthrough curve (C_t/C_o less than 0.15) [27]. Values of coefficients R^2 were lower than those in Thomas and Yoon–Nelson under the same experimental conditions. In this study, the breakthrough data obtained for color and COD were adequately described by the Thomas and Yoon–Nelson adsorption models.

5. Conclusion

The maximum adsorption capacities of color and COD in a fixed-bed column were found to be 100.15 Pt/Co and 73.23 mg/g, respectively at pH 4, initial concentration 486.87 Pt/Co color, and 251.65 mg/L of COD, flow rate of 10 mL/min and bed height 80 mm. The adsorption capacities of color and COD were found to increase with an increase in adsorbent dose and decrease with an increase in flow rate. The initial region of breakthrough curve was described by the Adams–Bohart model well at all experimental conditions studied while the transient stage or working stage of the breakthrough curve was described well by the Thomas and Yoon–Nelson models. Furthermore, error analysis showed that Yoon–Nelson and Thomas models were most suitable for the tracing of breakthrough curve at the experimental condition.

Acknowledgment

The authors acknowledge the research grant provided by University Science of Malaysia under the RU Grant Scheme that resulted in this article.

References

[1] L.I. Monser, N. Adhoum, Modified activated carbon for the removal of copper, zinc, chromium and cyanide from wastewater, Sep. Purif. Technol. 26 (2002) 137–146.
[2] A. Pela, E. Tokat, Color removal from cotton textile industry wastewater in an activated sludge system with various additives, Water Res. 36 (2002) 2920–2925.
[3] B.Y. Gao, Y. Wang, Q.Y. Yue, J.C. Wei, Q. Li, Color removal from simulated dye water and actual textile wastewater using a composite coagulant prepared by polyferric chloride and polydimethyldiallylammonium chloride, Sep. Purif. Technol. 54 (2007) 157–163.
[4] P. Kumar, B. Prasad, I.M. Mishra, Shri Chand Decolorization and COD reduction of dyeing wastewater from a cotton textile mill using thermolysis and coagulation, J. Hazard. Mater. 153 (2008) 635–645.
[5] H.R. Hitz, W. Huber, R.H. Reed, The adsorption of dyes on activated sludge, J. Soc. Dyers Colorists 94 (1978) 71–76.
[6] A.K. Mittal, S.K. Gupta, Biosorption of cationic dyes by dead macro-fungus *Fomitopsis carnea*: Batch studies, Water Sci. Technol. 34 (1996) 81–87.
[7] T.L. Hu, Removal of reactive dyes from aqueous solution by different bacteria genera, Water Sci. Technol. 34 (1996) 89–95.
[8] G. Skodras, I. Diamantopoulou, G. Pantoleontos, G.P. Sakellaropoulos, Kinetic studies of elemental mercury adsorption in activated carbon fixed bed reactor, J. Hazard. Mater. 158 (2008) 1–13.
[9] A.A. Ahmad, B.H. Hameed, Reduction of COD and color of dyeing effluent from a cotton textile mill by adsorption onto bamboo-based activated carbon, J. Hazard. Mater. 172 (2009) 1538–1543.
[10] M.J. Martin, A. Artola, M.D. Balaguer, M. Rigola, Activated carbons developed from surplus sewage sludge for the removal of dyes from dilute aqueous solutions, Chem. Eng. J. 94 (2003) 231–239.
[11] H. Denga, L. Yang, G. Tao, J. Dai, Preparation and characterization of activated carbon from cotton stalk by microwave assisted chemical activation—application in methylene blue adsorption from aqueous solution, J. Hazard. Mater. 166 (2009) 1514–1521.
[12] U. Kumar, M. Bandyopadhyay, Fixed bed column study for Cd(II) removal from wastewater using treated rice husk, J. Hazard. Mater. B 129 (2006) 253–259.

[13] D. Prahas, Y. Kartika, N. Indraswati, S. Ismadji, Activated carbon from jackfruit peel waste by H_3PO_4 chemical activation: Pore structure and surface chemistry characterization, Chem. Eng. J. 140 (2008) 32–42.
[14] I.A.W. Tan, A.L. Ahmad, B.H. Hameed, Adsorption of basic dye using activated carbon prepared from oil palm shell: Batch and fixed bed studies, Desalination 225 (2008) 13–28.
[15] B.H. Hameed, I.A.W. Tan, Nitric acid-treated bamboo waste as low-cost adsorbent for removal of cationic dye from aqueous solution, Desalin. Water Treat. 21 (2010) 357–363.
[16] E. Malkoc, Y. Nuhoglu, Y. Abali, Cr(VI) adsorption by waste acorn of *Quercus ithaburensis* in fixed beds: Prediction of breakthrough curves, Chem. Eng. J. 119 (2006) 61–68.
[17] D. Chatzopoulos, A. Varma, Aqueous-phase adsorption and desorption of toluene in activated carbon fixed beds: Experiments and model, Chem. Eng. Sci. 50 (1995) 127–141.
[18] A.J. Slaney, R. Bhamidimarri, Adsorption of pentachlorophenol (PCP) by activated carbon in fixed beds: Application of homogeneous surface diffusion model, Water Sci. Technol. 38 (1998) 227–235.
[19] A. Wolborska, External film control of the fixed bed adsorption, Chem. Eng. J. 73 (1999) 85–92.
[20] W.J. Weber, E.H. Smith, Simulation and design models for adsorption processes, Environ. Sci. Technol. 21 (1987) 1040–1050.
[21] B. Chen, C.W. Hui, G. McKay, Pore surface diffusion modeling for dyes from effluent on pith, Langmuir 17 (2001) 740–748.
[22] MDC Sdn.Bhd, Laws of Malaysia-Environmental Quality Act 1974 and Regulations, 4th edition, Kuala Lumpur, 1997.
[23] Standard Methods for the Analysis of Water and Wastewater, seventeenth ed., American Public Health Association (APHA), Washington DC, NY, USA, 1992.
[24] A.A. Ahmad, B.H. Hameed, A.L. Ahmad, Removal of disperse dye from aqueous solution using waste-derived activated carbon: Optimization study, J. Hazard. Mater. 170 (2009) 612–619.
[25] Z. Aksu, F. Gonen, Biosorption of phenol by immobilized activated sludge in a continuous packed bed: Prediction of breakthrough curves, Process Biochem. 39 (2004) 599–613.
[26] S.S. Baral, N. Das, T.S. Ramulu, S.K. Sahoo, S.N. Das, G. Roy Chaudhury, Removal of Cr(VI) by thermally activated weed *Salvinia cucullata* in a fixed-bed column, J. Hazard. Mater. 161 (2009) 1427–1435.
[27] G.C. Bohart, E.Q. Adams, Some aspect of the behavior of charcoal with respect to chlorine, J. Am. Chem. Soc. 42 (1920) 523–529.
[28] H.C. Thomas, Heterogeneous ion exchange in a flowing system, J. Am. Chem. Soc. 66 (1944) 1664–1666.
[29] Y.H. Yoon, J.H. Nelson, Application of gas adsorption kinetics 1 a theoretical model for respirator cartridge service time, Am. Ind. Hyg. Assoc. J. 45 (1984) 509–516.
[30] E. Valdman, L. Erijman, F.L.P. Pessoa, S.G.F. Leite, Continuous biosorption of Cu and Zn by immobilized waste biomass *Sargassum* sp., Process Biochem. 36 (2001) 869–873.
[31] A.A. Ahmad, B.H. Hameed, Fixed-bed adsorption of reactive azo dye onto granular activated carbon prepared from waste, J. Hazard. Mater. 175 (2010) 298–303.
[32] Z. Zulfadhly, M.D. Mashitah, S. Bhatia, Heavy metals removal in fixed-bed column by the macro fungus *Pycnoporus sanguineus*, Environ. Pollut. 112 (2001) 463–470.
[33] K. Vijayaraghavan, J. Jegan, K. Palanivelu, M. Velan, Removal of nickel(II) ions from aqueous solution using crab shell particles in a packed bed up flow column, J. Hazard. Mater. 113B (1–3) (2004) 223–230.
[34] R. Han, D. Ding, Y. Xu, W. Zou, Y. Wang, Y. Li, L. Zou, Use of rice husk for the adsorption of congo red from aqueous solution in column mode, Bioresour. Technol. 99 (2008) 2938–2946.
[35] R. Hana, Y. Wanga, X. Zhaoc, Y. Wanga, F. Xieb, J. Chengb, M. Tanga, Adsorption of methylene blue by phoenix tree leaf powder in a fixed-bed column: Experiments and prediction of breakthrough curves, Desalination 245 (2009) 284–297.
[36] G. McKay, Adsorption of dyestuffs from aqueous solution with activated carbon I: Equilibrium and batch contact time studies, J. Chem. Technol. Biotechnol. 32 (1982) 759–772.
[37] T.S. Singh, K.K. Pant, Equilibrium, kinetic and thermodynamics studies for adsorption of As(III) on activated alumina, Sep. Pur. Technol. 36 (2004) 139–147.